Theoretical and Biochemical Studies on the Selectivity of Nerve Growth Factor for Transition Metal Cations

Igor L. Shamovsky,[†,‡] Gregory M. Ross,[†,§] Richard J. Riopelle,[†,§] and Donald F. Weaver*[,†,‡]

Contribution from the Department of Medicine, Department of Chemistry, and Department of Pharmacology & Toxicology, Queen's University, Kingston, Ontario, Canada K7L 3N6

Received September 16, 1998. Revised Manuscript Received April 6, 1999

Abstract: Selective effects of transition metal cations (M^{n+}) on biological activities of nerve growth factor (NGF) have recently been described. It has been suggested that four residues in NGF (His^4, His^8, $His^{84'}$, and $Asp^{105'}$) form a distorted square base pyramidal coordination complex [$M(N{\cdot}His)_3(^-O_2C^{\gamma}{\cdot}Asp)$], thereby inducing a conformational transition within the NGF amino terminus (residues Ser^1-Phe^{12}), which constitutes a critical part of the receptor binding determinant. In this report, we provide theoretical and experimental data validating this structure and suggest a model for the selectivity of the M(II)−NGF interaction. The structures of the model complexes [$M(NH_3)_3(^-O_2CCH_3)$] and [$M(HNCH_2)_3(^-O_2CCH_3)$] (mimicking the M(II)−NGF coordination site) with first- and second-row divalent transition metal cations Co(II), Ni(II), Cu(II), Zn(II), Rh(II), Pd(II), and Cd(II) were studied by fully optimized ab initio molecular orbital calculations. Regardless of the chemical nature of the neutral ligands, these cations split into three groups: (i) Ni(II), Cu(II), and Pd(II) (d^8 and d^9 metals), which prefer a square pyramidal coordination; (ii) Co(II), Rh(II) (d^7 metals), and Zn(II) (the d^{10} first-row transition metal), which prefer a triangular bipyramidal environment; and (iii) Cd(II) (the d^{10} second-row transition metal), which has no intrinsic stereochemical preference. It should be noted, however, that stereochemical preferences of Cu(II) and Zn(II) are minor. Molecular mechanics calculations demonstrate that particular geometric features of the M(II)−NGF coordination site are most suitable for metal cations of intermediate sizes. Taken together with the intrinsic stereochemical preference of transition metal cations, three ions (Zn(II), Cu(II) and Pd(II)) are expected to be specific NGF antagonists, which is consistent with the effects of these ions on the conformation and biological activities of NGF.

Introduction

Nerve growth factor (NGF) is one member of a family of structurally and functionally related dimeric polypeptides (termed neurotrophins) which are essential for the development and maintenance of distinct neuronal populations in the central and peripheral nervous systems.[1−8] NGF is implicated in multiple neurologic disorders such as Alzheimer's disease,[9] epilepsy,[10,11] stroke,[12] and pain.[13] The biological functions of NGF are mediated by its interactions with two receptor types: TrkA, which belongs to the tyrosine kinase family and is specific for NGF, and $p75^{NTR}$, a member of the tumor necrosis factor (TNF) receptor superfamily, which binds all neurotrophins.[8,14−19] Although neurotrophin specificity is conventionally thought to result from the binding selectivity of Trk receptors,[8] recent experimental studies reveal important functional aspects of $p75^{NTR}$ (refs 19−27). The significance of the two-receptor recognition system for neurotrophins is poorly understood. In a variety of cell types, interaction of NGF with TrkA receptor mediates cell survival, whereas the NGF/$p75^{NTR}$ interaction may induce apoptosis (programmed cell death).[14,19,28−32] The allos-

* Corresponding author. Phone: (613) 533-6521. Fax: (613) 533-6669. E-mail: weaver@chem.QueensU.CA.

† Department of Medicine.

‡ Department of Chemistry.

§ Department of Pharmacology & Toxicology.

(1) Purves, D. *Body and Brain. A Trophic Theory of Neural Connectors*; Harvard University Press: Cambridge, MA, 1988.

(2) Snider, W. D.; Johnson, E. M. *Ann. Neurol.* **1989**, *26*, 489−506.

(3) Barde, Y.-A. *Neuron* **1989**, *2*, 1525−1534.

(4) Thoenen, H. *Trends Neurosci.* **1991**, *14*, 165−170.

(5) Korsching, S. *J. Neurosci.* **1993**, *13*, 2739−2748.

(6) Persson, H.; Ibáñez, C. F. *Curr. Opin. Neurol. Neurosurg.* **1993**, *6*, 11−18.

(7) Davies, A. M. *J. Neurobiol.* **1994**, *25*, 1334−1348.

(8) Ibáñez, C. F. *Trends Biotech.* **1995**, *13*, 217−227.

(9) Rylett, R. J.; Williams, L. R. *Trends Neurosci.* **1994**, *17*, 486-490.

(10) Ben-Ari, Y.; Represa, A. *Trends Neurosci.* **1990**, *13*, 312−318.

(11) Rashid, K.; Van der Zee, C. E. E. M.; Ross, G. M.; Chapman, C. A.; Stanisz, J.; Riopelle, R. J.; Fahnestock, M. *Proc. Natl. Acad. Sci. U.S.A.* **1995**, *92*, 9495−9499.

(12) Andsberg, G.; Kokaia, Z.; Björklund, A.; Lindvall, O.; Martínez-Serrano, A. *Eur. J. Neurosci.* **1998**, *10*, 2026−2036.

(13) McMahon, S. B.; Bennett, D. L. H.; Priestley, J. V.; Shelton, D. L. *Nature Med.* **1994**, *1*, 774−780.

(14) Barbacid, M. *J. Neurobiol.* **1994**, *25*, 1386-1403.

(15) Chao, M. V. *Cell* **1992**, *68*, 995−997.

(16) Chao, M. V. *Neuron* **1992**, *9*, 583−593.

(17) Kaplan, D. R.; Stephens, R. M. *J. Neurobiol.* **1994**, *25*, 1404−1417.

(18) Chao, M. V.; Hempstead, B. L. *Trends Neurosci.* **1995**, *18*, 321−326.

(19) Dechant, G.; Barde, Y.-A. *Curr. Opin. Neurobiol.* **1997**, *7*, 413−418.

(20) Heldin, C. H.; Ernlund, A.; Rorsman, C.; Rönnstrand, L. *J. Biol. Chem.* **1989**, *264*, 8905−8912.

(21) Jing, S.; Tapley, P.; Barbacid, M. *Neuron* **1992**, *9*, 1067−1079.

(22) Herrmann, J. L.; Menter, D. G.; Hamada, J.; Marchetti, D.; Nakajiama, M.; Nicolson, G. L. *Mol. Biol.* **1993**, *4*, 1205−1216.

(23) Barker, P. A.; Shooter, E. M. *Neuron* **1994**, *13*, 203-215.

(24) Dobrowsky, R.; Werner, M. H.; Castellino, A. M.; Chao, M. V.; Hannun, Y. A. *Science* **1994**, *265*, 1596−1599.

(25) Matsumoto, K.; Wada, R. K.; Yamashiro, J. M.; Kaplan, D. R.; Thiele, C. J. *Cancer Res.* **1995**, *55*, 1798−1806.

(26) Marchetti, D.; MsQuillan, D. J.; Spohn, W. C.; Carson, D. D.; Nicolson, G. L. *Cancer Res.* **1996**, *56*, 2856−2863.

(27) Ross, G. M.; Shamovsky, I. L.; Lawrance, G.; Solc, M.; Dostaler, S. M.; Weaver, D. F.; Riopelle, R. J. *Eur. J. Neurosci.* **1998**, *10*, 890−898.

10.1021/ja983303q CCC: $18.00
Published on Web 10/08/1999

teric interaction of these two receptors (when they are coexpressed) results in preferential TrkA-mediated survival over $p75^{NTR}$-mediated apoptosis.[27]

Direct interactions of Zn(II) and other transition metal cations with NGF and related neurotrophins, resulting in their inactivation, have recently been described.[33−35] Neurons may be exposed in vivo to significant concentrations of various transition metal cations. Two transition metal cations, Zn(II) and Cu(II), are both present in the brain in significant concentrations (∼100 μM).[36,37] Elevated levels of these metals arising from changes in their metabolism are found in pathological conditions such as cerebral ischemia,[38] epilepsy,[10] Alzheimer's disease,[36,37,39] Parkinson's disease,[40] amyotrophic lateral sclerosis,[40] and Wilson's disease. The ability of Zn(II) to modulate neuronal function[41] and modulate apoptosis[38] is well recognized. It has been suggested that Zn(II) exerts this important regulatory role at least in part by altering neurotrophin activity.[33] It has been further suggested that Zn(II) and Cu(II) directly bind to a specific coordination site within NGF, thereby altering the geometry of the receptor binding domains, which results in a loss of biological activities.[34] Consequently, aberrant concentrations of Zn(II) or Cu(II) in distinct populations of neurons supported by neurotrophins as survival factors may induce neuronal disorders by altering the desired biological outcomes of the neurotrophins.

It is recognized that Zn(II) plays two roles in metalloproteins: structural and catalytic.[42,43] In a proposed mechanism of Zn(II)-mediated NGF conformational change, Zn(II) exerts a structural role by maintaining a unique geometry of the coordination site.[33] The large majority of coordination sites in metalloproteins recognized as structural are found to contain either Ca(II) or Zn(II).[43] Since Ca(II) does not affect NGF activity[33] and considering the high concentrations of Zn(II) in brain,[41] we postulate that this site is particularly organized in nature for chelating Zn(II). Nevertheless, as observed in many experimental studies, Zn(II) ions can be replaced in metalloproteins by other transition metal cations such as Co(II), Cu(II), Ni(II), Hg(II), Mn(II), Fe(II), and Cd(II).[43−46] The metal cations Co(II) and Cd(II) most closely resemble Zn(II) in terms of stereochemical preference and size.[42,43,47−49] Surprisingly, different experimental studies on NGF conformation and biological activity have indicated that neither Co(II) nor Cd(II) is able to mimic the effects of Zn(II) on NGF, and only Cu(II) and Pd(II) ions behave similarly to Zn(II).[34,35] Further, it has been found that these three metal cations inhibit interactions of NGF with both TrkA and $p75^{NTR}$ receptors. Other transition metal cations have only partial activities at best; e.g. Ni(II) selectively blocks only the NGF/TrkA interaction. No transition metal cation which can specifically inhibit the NGF/$p75^{NTR}$ interaction without affecting the TrkA-mediated activities of NGF has been identified. Because of the significance of NGF in multiple neurologic disease processes and the unique selectivity of the NGF coordination site for transition metal cations, the determination of the structure of this site is an important and challenging problem.

In our model of the Zn(II)−NGF coordination site, the cation is chelated by four NGF residues, His^4 and His^8 of the first protomer and $His^{84'}$ and $Asp^{105'}$ of the second protomer, forming a five-coordinate site (two oxygen and three nitrogen atoms).[33] Although this particular coordination environment has been found in Zn(II)-containing proteins,[43,50−53] it is rather unusual, since Zn(II) generally forms a tetrahedral coordination as observed in the vast majority of metalloproteins.[42,43] The involvement of $His^{84'}$ and $Asp^{105'}$ in chelating Zn(II) has been established by X-ray crystallography of the NGFΔ1−8 deletion mutant in which the amino terminal residues Ser^1-His^8 were absent.[54] Furthermore, participation of the NGF amino terminal residues His^4 and His^8 in coordinating transition metal cations has been demonstrated by spectropolarimetry.[35] Nevertheless, predicted geometric features of the NGF metal coordination site remain hypothetical. Although transition metal cations have been used in X-ray analysis to resolve the structure of NGF, they do not eliminate conformational flexibility inherent in the NGF termini,[55,56] suggesting crystal structures of the complexes of NGF with transition metal cations involving the amino terminus may not presently be obtained. Consequently, the structure of the coordination site within NGF should be determined alternatively by spectroscopic and theoretical methods.

In this report, we investigate the interactions of transition metal cations with NGF. As demonstrated by chemical cross-linking of NGF protomers, Zn(II), Cu(II), and Pd(II) change NGF conformation whereas Co(II) and Cd(II) do not. This striking selectivity of NGF is explained by a model developed based on results of computational studies. The structures of the

(28) Rabizadeh, S.; Oh, J.; Zhong, L. T.; Yang, J.; Bitler, C. M.; Butcher, L. L.; Bredesen, D. E. *Science* **1993**, *261*, 345−348.
(29) Barrett, G. L.; Bartlett, P. F. *Proc. Natl. Acad. Sci. U.S.A.* **1994**, *91*, 6501−6505.
(30) Van der Zee, C. E. E. M.; Ross, G. M.; Riopelle, R. J.; Hagg, T. *Science* **1996**, *274*, 1729−1732.
(31) Carter, B. D.; Lewin, G. R. *Neuron* **1997**, *18*, 187−190.
(32) Frade, J. M.; Barde, Y.-A. *Neuron* **1998**, *20*, 35−41.
(33) Ross, G. M.; Shamovsky, I. L.; Lawrance, G.; Solc, M.; Dostaler, S. M.; Jimmo, S. L.; Weaver, D. F.; Riopelle, R. J. *Nature Med.* **1997**, *3*, 872−878.
(34) Wang, W.; Post, J. I.; Dow, K. E.; Shin, S. H.; Riopelle, R. J.; Ross, G. M. *Neurosci. Lett.* **1999**, *259*, 115−118.
(35) Ross, G. M.; Shamovsky, I. L.; Wang, W.; Solc, M.; Lawrance, G.; Dostaler, S. M.; Riopelle, R. J. Submitted.
(36) Lovell, M. A.; Robertson, J. D.; Teesdale, W. J.; Campbell, J. L.; Markesbery, W. R. *J. Neurol. Sci.* **1998**, *158*, 47−52.
(37) Atwood, C. S.; Moir, R. D.; Huang, X.; Scarpa, R. C.; Bacarra, N. M. E.; Romano, D. M.; Hartshorn, M. A.; Tanzi, R. E.; Bush, A. I. *J. Biol. Chem.* **1998**, *273*, 12817−12826.
(38) Koh, J.-Y.; Suh, S. W.; Gwag, B. J.; He, Y. Y.; Hsu, C. Y.; Chi, D. W. *Science* **1996**, *272*, 1013−1016.
(39) Bush, A. I.; Pettingell, W. H.; Multhaup, G.; Paradis, M. D.; Vonsattel, J.-P.; Gusella, J. F.; Beyreuther, K.; Masters, C. L.; Tanzi, R. E. *Science* **1993**, *265*, 1464−1467.
(40) Cuajungco, M. P.; Lees, G. J. *Neurobiol. Disease* **1997**, *4*, 137−169.
(41) Harrison, N. L.; Gibbons, S. J. *Neuropharmacol.* **1994**, *33*, 935−952.
(42) Regan, L.; Clarke, N. D. *Biochemistry* **1990**, *29*, 10878−10883.
(43) Holm, R. H.; Kennepohl, P.; Solomon, E. I. *Chem. Rev.* **1996**, *96*, 2239−2314.
(44) Holmquist, B.; Valee, B. L. *J. Biol. Chem.* **1974**, *249*, 4601−4607.
(45) Gomis-Rüth, F.-X.; Grams, F.; Yiallouros, I.; Nar, H.; Küsthardt, U.; Zwilling, R.; Bode, W.; Stöcker, W. *J. Biol. Chem.* **1994**, *269*, 17111−17117.
(46) Holland, D. R.; Hausrath, A. C.; Juers, D.; Mattheus, B. W. *Protein Sci.* **1995**, *4*, 1955−1965.
(47) Green, L. M.; Berg, J. M. *Proc. Natl. Acad. Sci.* **1989**, *86*, 4047−4051.
(48) Kochoyan, M.; Keutmann, H. T.; Weiss, M. A. *Biochemistry* **1991**, *30*, 9396−9402.
(49) Auld, D. S. *Methods Enzymol.* **1995**, *248*, 228−242.
(50) Argos, P.; Garavito, R. M.; Eventoff, W.; Rossmann, M. G. *J. Mol. Biol.* **1978**, *126*, 141−158.
(51) Spurlino, J. C.; Smith, D. L. *Protein Data Bank*; Brookhaven National Laboratory: Upton, NY; accession code 1HFC.
(52) Stams, T.; Spurlino, J. C.; Smith, D. L.; Rubin, B. *Protein Data Bank*; Brookhaven National Laboratory: Upton, NY; accession code 1MNC.
(53) Zhang, D.; Botos, I.; Gomis-Rüth, F.-X.; Doll, R.; Blood, C.; Njoroge, F. G.; Fox, J. W.; Bode, W.; Meyer, E. F. *Protein Data Bank*; Brookhaven National Laboratory: Upton, NY; accession code 1ATL.
(54) Holland, D. R.; Cousens, L. S.; Meng, W.; Matthews, B. W. *J. Mol. Biol.* **1994**, *239*, 385−400.
(55) McDonald, N. Q.; Lapatto, R.; Murray-Rust, J.; Gunning, J.; Wlodawer, A.; Blundell, T. L. *Nature* **1991**, *354*, 411−414.
(56) Bax, B.; Blundell, T. L.; Murray-Rust, J.; McDonald, N. Q. *Structure* **1997**, *5*, 1275−1285.

coordination site of NGF with first- and second-row transition metal cations Co(II), Ni(II), Cu(II), Zn(II), Rh(II), Pd(II), and Cd(II) are simulated by ab initio and molecular mechanics calculations. It is demonstrated that both stereochemistry and size of the coordination site are most consistent with Zn(II), Cu(II), and Pd(II).

Methods

Protomer Cross-Linking of NGF. NGF has two identical protomers, each having a molecular weight of approximately 13 kDa. The chemical cross-linking agent bis-sulfosuccinimidyl-suberate (BS^3) forms covalent bonds with two functional groups (likely primary amines) belonging to different protomers of NGF, thereby connecting them into a covalently coupled dimer with a molecular weight of about 26 kDa. This reaction is sensitive to the distance between the functional groups, which is dependent on NGF conformation. Consequently, those compounds which influence NGF conformation may also affect the ability of BS^3 to cross-link NGF protomers. Since NGF is a rather rigid molecule with only its amino (Ser^1 to Ser^{13}) and carboxyl ($Leu^{112'}$ to $Arg^{118'}$) termini being flexible domains,[54−56] significant conformational changes are most probable within these terminal regions. Thus, changes in cross-linking of NGF protomers is closely related to changes in mutual orientation of the juxtaposed amino and carboxyl termini.[57,58] While the ability of a metal ion to alter protomer cross-linking efficiency indicates a change in NGF conformation, it offers no insight into what the new conformation is.

For experimental studies on the alterations of the NGF conformation, 0.1 nM ^{125}I-labeled NGF was incubated in the presence or absence of transition metal cations Co(II), Ni(II), Cu(II), Zn(II), Pd(II), and Cd(II) (100 μM of their Cl salts) in HKR buffer (10 mM HEPES [pH 7.35] containing 125 mM NaCl, 4.8 mM KCl, 1.3 mM $CaCl_2$, 1.2 mM $MgSO_4$, 1.2 mM KH_2PO_4, 1 g/L glucose, 1 g/L BSA) for 2 h at 4 °C in a total volume of 0.1 mL.[33] Chloride salt of each metal ion was used (either anhydrous or hydrated); it was dissolved in DMSO at a concentration of 100 mM and then diluted in a HKR buffer to a final concentration of 100 μM. For cross-linking NGF protomers, 0.4 mM BS^3 was added and the mixture was incubated for 30 min at 25 °C. The reaction was quenched with reducing SDS PAGE (sodium dodecyl sulfate polyacrylamide gel electrophoresis) sample buffer, electrophoresed using a 15% acrylamide gel, and processed for autoradiography.

Ab Initio Calculations. The putative coordination site $[M(N\cdot His)_3(^-O_2C^{\gamma}\cdot Asp)]$ of NGF was simulated with two model complexes, $[M(NH_3)_3(^-O_2CCH_3)]$ (complex **I** with sp^3-hybridized nitrogen atoms) and $[M(HNCH_2)_3(^-O_2CCH_3)]$ (complex **II** with sp^2-hybridized nitrogen atoms), in which ammonia or methanimine molecules mimic neutral His residues, and a bidentate acetate anion mimics negatively charged Asp. The methylene groups within the methanimine molecules of complex **II** were oriented toward the acetate anion to avoid possible artifactual NH···OC hydrogen bonding. Divalent transition metal cations (M = Co(II), Ni(II), Cu(II), Zn(II), Rh(II), Pd(II), and Cd(II)) were described by relativistic compact effective potentials,[59] which explicitly consider the electrons in the $(n-1)s(n-1)p(n-1)dns$ shells. All-electron 6-31+G* basis sets were utilized for H, C, N, and O atoms, in which the split valence 6-31G basis sets[60] were augmented by diffuse sp functions[61] and polarization six-component Cartesian d functions on atoms C, N, and O.[62] The importance of diffuse functions has been demonstrated for describing the electronic structure of anions.[63,64] Electron correlation was taken into account by the density functional theory (DFT) method[65,66] using Becke's three-parameter exchange functional with the Lee−Yang−Parr's correlation functional (B3LYP).[67] Geometries of the model complexes were fully optimized at the Hartree−Fock (HF) and the DFT levels of theory, and the reliability of the optimized structures as corresponding to the true energy minima was proven by computations of normal frequencies. Single-point energies of the optimized structures were then calculated at higher levels of theory using the 6-311G(2df,2pd) extended basis sets for atoms H, C, N, and O.[62] Ab initio calculations were performed with the Gaussian-94 program.[68]

Molecular Modeling. The aim of the molecular modeling studies was to predict factors which affect the integrity of the coordination site $[M(N\cdot His)_3(^-O_2C^{\gamma}\cdot Asp)]$ within NGF, rather than to identify its structural features. Molecular modeling was used in conjunction with ab initio methods, since methods of bioinorganic molecular mechanics are not yet sufficiently developed to provide reliable structural predictions, particularly for metalloproteins with transition metal cations.[69] The three-dimensional structures of the complexes of NGF with selected transition metal cations (M = Ni(II), Cu(II), Zn(II), Pd(II), and Cd(II)) were obtained by molecular mechanics calculations based on the X-ray crystallographic structure of mouse NGF[54,55] and on the geometry of the Zn(II) coordination site as revealed by recent molecular dynamics simulations.[33] Potential energies of the complexes were calculated within the framework of the all-atom CHARMM force field model.[70] Potential energy minimizations were performed with QUANTA-97 molecular modeling software.[71] In addition to the three-dimensional coordinates of the chelated metal cation, the conformational parameters of the following residues of NGF involved in formation of the coordination site were taken into account when minimizing potential energies of the complexes:[33] Ser^1 to Ser^{13} (amino terminus of NGF), $Leu^{112'}$ to $Arg^{118'}$ (juxtaposed carboxyl terminus of NGF), and six additional residues located in a close proximity to the coordination site $Thr^{29'}$, $Glu^{35'}$, $His^{84'}$, $Phe^{86'}$, $Arg^{103'}$, and $Asp^{105'}$. Positions of all other atoms of NGF were fixed at their X-ray crystallographic coordinates.[55]

Results and Discussion

Protomer Cross-Linking of NGF. The ability of transition metal cations to change NGF conformation was evaluated by their ability to inhibit cross-linking of NGF protomers using the cross-linking agent BS^3 as presented in Figure 1. Cations Cu(II), Zn(II), and Pd(II) considerably reduced protomer cross-linking efficiency, which indicates that these ions bind to NGF and change its conformation. The other cations tested (Co(II), Ni(II), and Cd(II)) were inactive. This result demonstrates a unique selectivity of the coordination site within NGF which has not been previously reported. Specifically, the NGF coordination site is able to distinguish Zn(II) from Co(II) and Cd(II), which behave very similarly in the vast majority of metalloproteins.[42,43,47−49]

Ab Initio Calculations. Molecular systems with transition metal cations having different spin states (Co(II), Ni(II), Rh-

(57) Shamovsky, I. L.; Ross, G. M.; Riopelle, R. J.; Weaver, D. F. *J. Am. Chem. Soc.* **1996**, *118*, 9743−9749.
(58) Shamovsky, I. L.; Ross, G. M.; Riopelle, R. J.; Weaver, D. F. *Can. J. Chem.* **1998**, *76*, 1389−1401.
(59) Stevens, W. J.; Krauss, M.; Basch, H.; Jasien, P. G. *Can. J. Chem.* **1992**, *70*, 612−630.
(60) Hariharan, P. C.; Pople, J. A. *Theor. Chim. Acta* **1973**, *28*, 213−222.
(61) Clark, T.; Chandrasekhar, J.; Spitznagel, G. W.; Schleyer, P.v. R. *J. Comput. Chem.* **1983**, *4*, 294−301.
(62) Frisch, M. J.; Pople, J. A.; Binkley, J. S. *J. Chem. Phys.* **1984**, *80*, 3265−3269.
(63) Chandrasekhar, J.; Andrade, J. G.; Schleyer, P.v. R. *J. Am. Chem. Soc.* **1981**, *103*, 5609−5612.
(64) Chandrasekhar, J.; Andrade, J. G.; Schleyer, P.v. R. *J. Am. Chem. Soc.* **1981**, *103*, 5612−5614.
(65) Parr, R. F.; Yang, W. *Density Functional Theory of Atoms and Molecules*; Oxford University: New York, 1989.
(66) *Density Functional Methods in Chemistry*; Labanowski, J. K., Andzelm, J. W., Eds.; Springer-Verlag: New York, 1991.
(67) Becke, A. D. *J. Chem. Phys.* **1993**, *98*, 5648−5652.
(68) Frisch, M. J.; Trucks, G. W.; Schlegel, H. B.; Gill, P. M. W.; Johnson, B. G.; Robb, M. A.; Cheeseman, J. R.; Keith, T.; Petersson, G. A.; Montgomery, J. A.; Raghavachari, K.; Al-Laham, M. A.; Zakrzewski, V. G.; Ortiz, J. V.; Foresman, J. B.; Cioslowski, J.; Stefanov, B. B.; Nanayakkara, A.; Challacombe, M.; Peng, C. Y.; Ayala, P. Y.; Chen, W.; Wong, M. W.; Andres, J. L.; Replogle, E. S.; Gomperts, R.; Martin, R. L.; Fox, D. J.; Binkley, J. S.; Defrees, D. J.; Baker, J.; Stewart, J. P.; Head-Gordon, M.; Gonzalez, C.; Pople, J. A. *Gaussian-94*, revision E.2.; Gaussian, Inc.: Pittsburgh, PA, 1995.
(69) Zimmer, M. *Chem. Rev.* **1995**, *95*, 2629−2649.
(70) Brooks, B. R.; Bruccoleri, R. E.; Olason, B. D.; States, D. J.; Swaminathan, S.; Karplus, M. *J. Comput. Chem.* **1983**, *4*, 187−217.
(71) Molecular Simulations, Inc.: San Diego, CA.

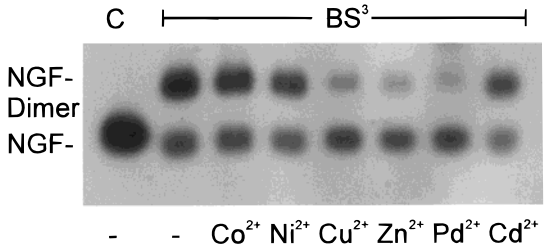

Figure 1. Changes in the conformation of NGF as demonstrated by reduced ability of the cross-linking agent BS^3 to covalently cross-link NGF monomers in the presence of indicated transition metal cations. In control experiment (C), no cross-linking agent was added and, correspondingly, no NGF covalent dimer was observed. Metals Cu(II), Zn(II), and Pd(II) significantly reduce the ability of BS^3 to covalently cross-link $^{125}I-NGF$.

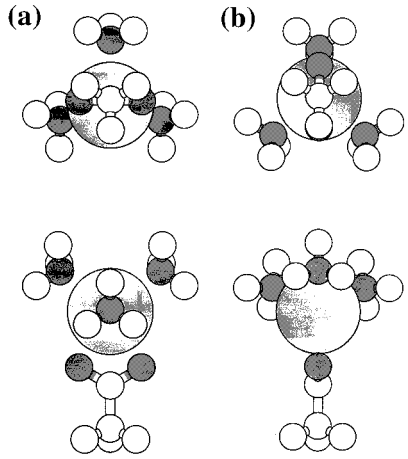

Figure 2. Orthogonal projections of the fully optimized geometries of the $[M(NH_3)_3(^-O_2CCH_3)]$ coordination complexes of divalent transition metal cations (M) obtained at the B3LYP/6-31+G* level of theory. (a) Distorted square pyramidal geometry characteristic for M = Ni(II), Cu(II), and Pd(II) (structure **I-A**); (b) triangular bipyramidal geometry characteristic for M = Co(II), Rh(II), Zn(II), and Cd(II) (structure **I-B**). Chelating atoms of the ligand molecules are illustrated by small dark-grey spheres, transition metal cations by large light-grey spheres.

(II), and Pd(II)) appeared to be more stable at the high-spin state (data not shown); accordingly, the high-spin states were presumed in all calculations describing those metals. Geometry optimizations of the coordination complex **I** at the HF/6-31+G* and B3LYP/6-31+G* levels indicate that there are two types of the minimal energy structures, **I-A** and **I-B**, each possessing C_s point-group symmetry. Structure **I-A** with a distorted square pyramidal geometry is inherent in complexes with M = Ni(II), Cu(II), and Pd(II). In this structure (Figure 2a), four coordinating atoms (both carboxylate oxygens of an acetate and the nitrogens of two ammonia molecules) lie in the same plane, with the fifth coordinating atom (nitrogen of the third ammonia) "hanging over" and pulling the metal cation out of the plane. Structure **I-B** with a triangular bipyramidal geometry is characteristic for M = Co(II), Zn(II), Rh(II), and Cd(II). In this structure (Figure 2b), two ammonia molecules are located symmetrically with respect to the plane formed by the carboxyl group, the metal cation and the nitrogen atom of the third ammonia. As seen in Figure 2, both of these structures are five-coordinate, and the main difference between them is the orientation of the bidentate carboxyl group. In structure **I-B**, this group is turned by 90° with respect to its orientation in structure **I-A**.

The coordination complex **I** has only one minimal energy structure, either **I-A** or **I-B,** depending on the particular stereochemical preference of the chelated transition metal cation. The second structure always corresponds to a saddle-point with two imaginary frequencies. Table 1 presents relative energies of the two structures for each metal cation at the HF/6-31+G*, B3LYP/6-31+G*, HF/6-311G(2df,2pd)//HF/6-31+G*, and B3LYP/6-311G(2df,2pd)//B3LYP/6-31+G* levels of theory. As seen, the stereochemical preference of Zn(II) and Cd(II) (d^{10} elements) for structure **I-B** is insignificant at all levels, since these particular metals have completely occupied d orbitals and are thus spherically symmetrical. On the contrary, all other metals have a definite stereochemical preference. Metals of the d^8 (Ni(II) and Pd(II)) and d^9 (Cu(II)) groups are more likely to adopt structure **I-A**, whereas d^7 metals (Co(II) and Rh(II)) prefer structure **I-B**. The stereochemical preference of the transition metal cation is determined solely by the occupancy of its three highest d-orbitals. With the exception of Cd(II), if the levels are equally occupied, the metal cation adopts coordination **I-B**, otherwise it prefers square pyramidal coordination **I-A**.

Geometry optimizations of the complex **II** at the Hartree−Fock level were unsuccessful for all open-shell structures because of poor convergence properties of the self-consistent field procedure. On the other hand, electron correlation has completely eliminated this problem, hence further discussion of the geometric features of complex **II** is based exclusively on the B3LYP/6-31+G* optimized structures. The minimal energy structures of the complex **II** (Figure 3) are strikingly similar to those of the complex **I** (Figure 2). The square pyramidal coordination geometry (structure **II-A**) remains to be the most stable for metals of the d^8 and d^9 groups, whereas the triangular bipyramidal structure **II-B** is the only minimum for metals of the d^7 and d^{10} groups. A specific feature of the complex **II** is that the structure **II-B** with the triangular bipyramidal geometry corresponds to the local energy minimum for the d^8 and d^9 metals, as demonstrated by computations of normal frequencies. The stabilization of the **II-B** structure for the d^8 and d^9 metals results in decreasing the energy gap between the **II-A** and **II-B** structures with respect to the gap between structures **I-A** and **I-B** (Table 1). Because of this stabilization, preference of Cu(II) for the **II**−**A** structure is minor. It was not possible to calculate the corresponding energy gap for the d^7 or d^{10} metals, since with these metals geometry optimization of **II-A** always converged to **II-B**. Consistent with published experimental and theoretical data, the most stable configuration of all the model structures corresponds to a coplanar location of metal cation with planar ligands (such as acetate anion or methanimine), with the carboxylic group being in bidentate coordination.[43,72−76]

Optimal spacial positions of the ligands around the metal atom in the complexes **I** and **II** were expressed by spherical coordinates of the coordinating atoms, namely r (radius), θ (latitude), and φ (longitude). Metal−ligand separations (r) are presented in Table 2. Orientations of metal−ligand bonds (θ versus φ) are illustrated in Figure 4. As seen in Table 2, the metal−ligand bond lengths M−N(sp^2) are shorter than M−N(sp^3) roughly by 0.04 Å. This bond length decrease caused by the alterations in hybridization of one of the two atoms of the bond is well-known in other systems (e.g., compare with the 0.04 Å bond length decrease when going from C(sp^3)−C(sp^3) to

(72) Carrell, C. J.; Carrell, H. L.; Erlebacher, J.; Glusker, J. P. *J. Am. Chem. Soc.* **1988**, *110*, 8651−8656.
(73) Christianson, D. W. *Adv. Protein Chem.* **1991**, *42*, 281−355.
(74) Glusker, J. P. *Adv. Protein Chem.* **1991**, *42*, 1−76.
(75) Leban, I.; Šegedin, P.; Gruber, K. *Acta Crystallogr.* **1996**, *C52*, 1096−1098.
(76) Hoang, N. N.; Valach, F.; Dunaj-Jurčo, M. *Acta Crystallogr.* **1995**, *C51*, 1095−1097.

Table 1. Relative ab Initio Energies (in kJ/mol) of Two Structures, A (Square Pyramidal) and B (Triangular Bipyramidal), of the Pentacoordinated Complexes $[M(NH_3)_3(^-O_2CCH_3)]$ (Complex I) and $[M(HNCH_2)_3(^-O_2CCH_3)]$ (Complex II) of Divalent Transition Metal Cations (M)[f]

		first-row transition metals				second-row transition metals		
structure	level	Co(II)	Ni(II)	Cu(II)	Zn(II)	Rh(II)	Pd(II)	Cd(II)
				Complex **I**				
I-A	HF/B1[a,b]	9.79	**0.00**	**0.00**	2.01	14.69	**0.00**	**0.00**
	HF/B2[a,c]	10.50	**0.00**	**0.00**	2.85	18.54	**0.00**	0.04
	B3LYP/B1[d]	20.59	**0.00**	**0.00**	2.64	26.69	**0.00**	**0.00**
	B3LYP/B2[d]	20.17	**0.00**	**0.00**	3.85	26.57	**0.00**	0.63
I−B	HF/B1[a]	**0.00**	5.69	3.39	**0.00**	**0.00**	15.10	0.54
	HF/B2[a]	**0.00**	6.36	4.56	**0.00**	**0.00**	16.32	**0.00**
	B3LYP/B1[d]	**0.00**	8.54	3.64	**0.00**	**0.00**	20.25	0.33
	B3LYP/B2[d]	**0.00**	7.32	4.73	**0.00**	**0.00**	22.80	**0.00**
				Complex **II**				
II-A	B3LYP/B1[d]	N/D	**0.00**	**0.00**	N/D	N/D	**0.00**	N/D
	B3LYP/B3[d,e]	N/D	**0.00**	**0.00**	N/D	N/D	**0.00**	N/D
II−B	B3LYP/B1[d]	**0.00**	4.56	0.92	**0.00**	**0.00**	12.97	**0.00**
	B3LYP/B3[d]	**0.00**	4.61	1.07	**0.00**	**0.00**	12.46	**0.00**

[a] Geometries of the complexes were fully optimized at the HF/6-31+G* level. [b] B1 denotes the 6-31+G* basis set. [c] B2 denotes the 6-311G(2df,2pd) basis set which was used only for single-point calculations. [d] Geometries were fully optimized at the B3LYP/6-31+G* level. [e] B3 denotes the 6-311G(2d,2p) basis set. [f] N/D, not determined because of convergence to the **II-B** structure. The most stable structures are highlighted in bold for clarity.

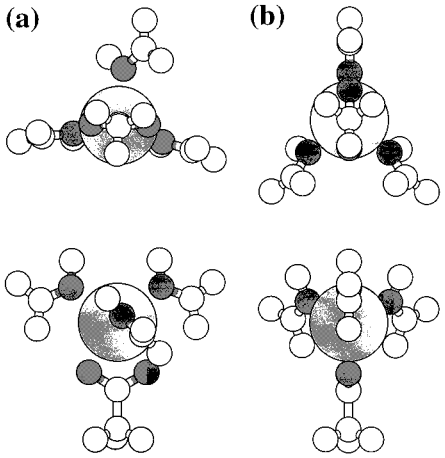

Figure 3. Orthogonal projections of the fully optimized geometries of the $[M(HNCH_2)_3(^-O_2CCH_3)]$ coordination complexes of divalent transition metal cations (M) obtained at the B3LYP/6-31+G* level of theory. (a) Distorted square pyramidal geometry characteristic for M = Ni(II), Cu(II), and Pd(II) (structure **II-A**); (b) triangular bipyramidal geometry characteristic for M = Co(II), Rh(II), Zn(II), and Cd(II) (structure **II-B**).

Table 2. Average Metal−Ligand Bond Lengths (in Å) in the Most Stable Structures of the Pentacoordinated Complexes $[M(NH_3)_3(^-O_2CCH_3)]$ (Complex I) and $[M(HNCH_2)_3(^-O_2CCH_3)]$ (Complex II) of Divalent Transition Metal Cations (M) Obtained by Fully Optimized ab Initio Calculations at the B3LYP/6-31+G* Level

	first-row transition metals				second-row transition metals		
bond	Co(II)	Ni(II)	Cu(II)	Zn(II)	Rh(II)	Pd(II)	Cd(II)
			Complex **I**				
M−N	2.121	2.098	2.133	2.116	2.286	2.282	2.357
M−O	2.138	2.058	2.028	2.165	2.285	2.233	2.311
average	2.128	2.082	2.091	2.136	2.286	2.262	2.339
			Complex **II**				
M−N	2.084	2.055	2.098	2.099	2.229	2.227	2.327
M−O	2.149	2.072	2.037	2.158	2.312	2.242	2.332
average	2.110	2.062	2.074	2.123	2.262	2.233	2.329

$C(sp^3)-C(sp^2)$). Positions of the optimal orientations of metal−ligand bonds in both square pyramidal (Figure 4a) and triangular bipyramidal (Figure 4b) environments are determined by the type of metal atom, rather then by the type of ligand. Thus, regardless of the chemical nature of neutral ligands, positions of the equatorial bonds split into two clusters according to the occupancy of three highest d orbitals of metal cations: Co(II), Zn(II), Rh(II), and Cd(II) with equivalent, and Ni(II), Cu(II), and Pd(II) with nonequivalent occupancy. These observations suggest that π-orbitals of methanimine do not participate in bonding to the metal cations, which is consistent with previous studies which indicated that neutral ligands behave mostly as σ donors.[43] This implies that metals with nonequivalent occupancy of the three highest d orbitals possess an "intrinsic desire" to have any four of their ligands arranged in a square, which agrees well with crystallographic data,[43,75,76] including the observation that Pd(II) is typically found in a square planar coordination. Thus, neutral ligands do not directly affect the stereochemical preference of the coordinated transition metal cations, even though this preference might be very minor, as found for Cu(II) and Zn(II).

As seen in Figures 2 and 3, the energy minimum structures of the complexes possess C_s symmetry, except for the **II-A** structure (Figure 3a) which has no symmetry elements. In this particular coordination state, the plane of the axial ligand, instead of being coplanar with the plane of symmetry (which exists in the corresponding structure **I-A**), forms an angle of approximately 45° with it for all d^8 and d^9 metals. This deviation can be easily explained by electron repulsion of doubly occupied orbitals of metal and axial ligand (Figure 5). The two lowest fully occupied d-orbitals (d_{xz} and d_{yz}) of a transition metal, being in a square pyramidal coordination state, create a four-fold hindering for torsional rotation of the axial ligand around the *Z* axis, i.e., around the single M−N bond. Because of spatial location and symmetry of the other three d orbitals of the metal, d_{xy}, $d_{x^2-y^2}$, and d_{z^2}, they do not create any hindrances to the rotation of the axial ligand. Electron repulsion of orbitals d_{xz} and d_{yz} of a transition metal from three torsional electron pairs of an axial nitrogen atom (represented either by three σ orbitals in ammonia or by two σ and one π orbitals in methanimine) causes particular conformational preferences of the axial ligand in the square pyramidal coordination states. In the complex **I** with a tetrahedral nitrogen, the minimal energy structure corresponds to a symmetric eclipsed conformation (Figure 5a). On the other hand, in the complex **II** with a trigonal nitrogen,

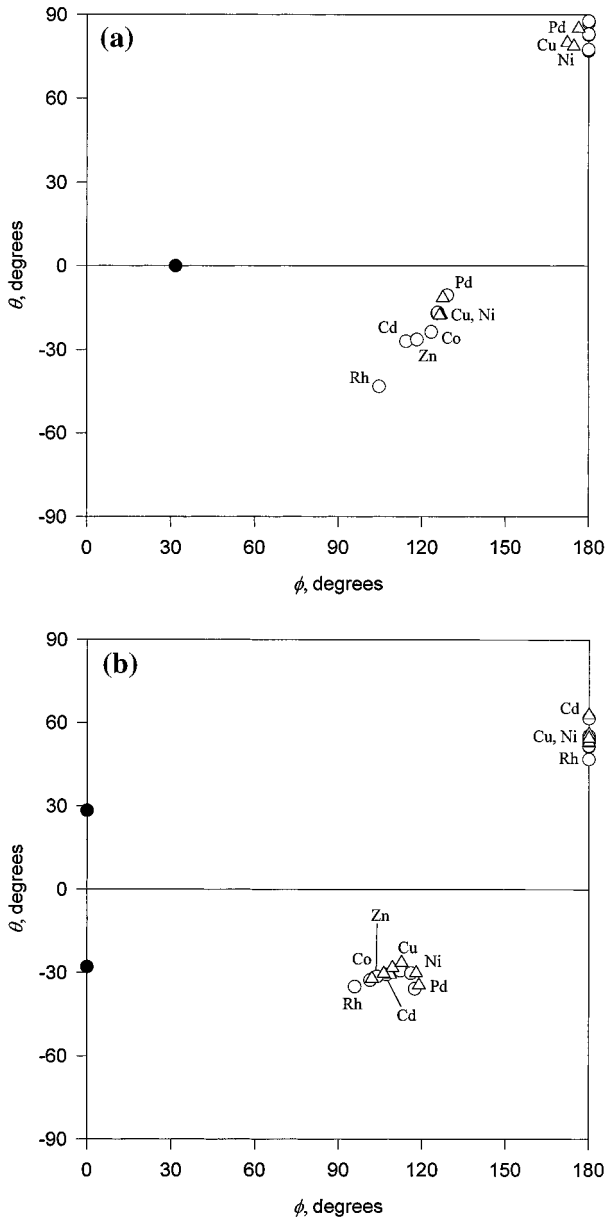

Figure 4. Optimal sites of ligands around the pentacoordinated divalent transition metal cations in the square pyramidal (a) and triangular bipyramidal (b) coordination environments obtained by fully optimized correlated relativistic DFT calculations at the B3LYP/6-31+G* level. Spherical coordinates θ (latitude) and φ (longitude) of oxygen and nitrogen atoms of the ligands were calculated assuming that the equator is perpendicular to the plane of symmetry and passes through carbon of carboxyl group which also defines "zero" of longitude. Only one of the two symmetric semispheres is shown ($0° < \varphi < 180°$). For three asymmetric structures **II-A**, the coordinate system was defined by the least-squares method. Empty circles and triangles denote model complexes **I** and **II**, respectively. Black circles designate the sites of carboxyl oxygens.

this repulsion results in an asymmetric staggered conformation in which a plane of the axial ligand is coplanar with the diagonal of the square (Figure 5b). It is important to note that the origin of torsional barriers of the axial ligand does not depend either on the chemical nature or conformation of equatorial ligands, or on occupancy of higher d orbitals of metal. This being the case, the depicted conformational features of the axial ligands (Figure 5) should be inherent in other molecular systems with transition metal cations located in a square pyramidal or octahedral coordination environment, regardless of nature of

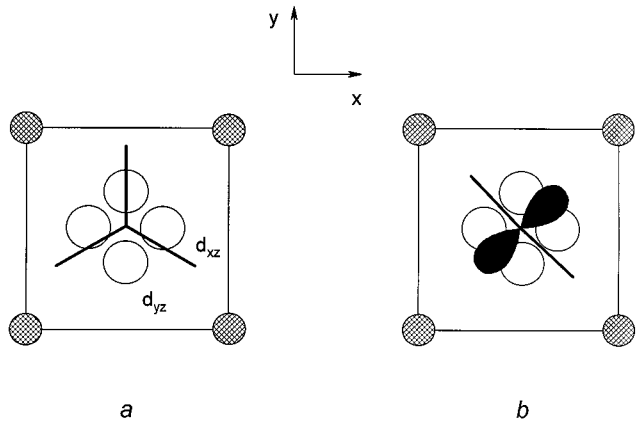

Figure 5. General structure of the square pyramidal coordination states, and the explanation for the conformational preferences of axial ligands in structures **I-A** and **II-A** based on the origin of hindrances to torsional rotation of the axial ligand around the *Z*-axis in a square pyramidal or octahedral coordination environment: (a) Most stable conformation of the **I**−**A** structure inherent in the complex **I** with tetrahedral axial ligand and transition metal cations of d^8 or d^9 group; (b) most stable conformation of the **II**−**A** structure characteristic for the complex **II** with trigonal axial ligand and transition metal cations of d^8 or d^9 group. General location of equatorial ligands is illustrated by double-hatched circles, electron density of d_{xz} and d_{yz} orbitals around the metal−ligand bond by empty circles, σ-bonds of an axial nitrogen atom by solid lines, p-orbital of an axial nitrogen atom by black 8-shaped figure.

equatorial ligands or occupancy of three higher d orbitals of transition metal or its valence state (provided the two lower d orbitals remain occupied). Available X-ray crystallographic data deposited in the Brookhaven Protein Data Bank on natural metalloproteins confirm this point and indicate that the observed conformation of the axial His residue in square pyramidal or octahedral complexes of transition metal cations is indeed similar to that of axial methanimine in the **II-A** structure (compare Figures 6 and 5b). Surprisingly, a barrier hindering the rotation of the axial ligand in the complex **II** appears to be low (3−4 kJ/mol at the B3LYP/6-311G(2d,2p)//B3LYP/6-31+G* level), which implies that energy of coordination sites in natural metalloproteins has been carefully regulated during evolution, such that rather small stereochemical preference of transition metal cations (Table 1) represents an important factor for a proper function of metal coordination sites.[43]

Since transition metal cations display low affinity for NGF,[33] the function of the NGF coordination site is expected to be particularly sensitive; therefore, the intrinsic stereochemical preference of the transition metal cations revealed by ab initio calculations (Table 1) seem to be sufficient to account for selectivity of the NGF coordination site. As shown in Table 1, intrinsic stereochemical preference of the transition metal cations of the d^7−d^9 groups becomes more apparent with a decreasing number of d electrons and is more pronounced for the second- than for the first-row transition metals. However, the carboxylate anion of $Asp^{105'}$ in NGF may be sufficiently flexible to switch the stereochemical environment of the coordination site to satisfy the intrinsic preference of the particular cation. To evaluate this possibility, conformational flexibility of the isolated propionate anion was studied with ab initio calculations at the HF/6-31+G*, B3LYP/6-31+G*, HF/6-311G(2df,2pd)//HF/6-31+G*, and B3LYP/6-311G(2df,2pd)//B3LYP/6-31+G* levels. The minimal energy structure corresponds to the C−O/C−C eclipsed conformation at all of the considered levels of theory. Hindrances to rotation of the carboxylate anion obtained at these levels are 3.01, 2.93, 4.06, and 4.85 kJ/mol, respectively, which demon-

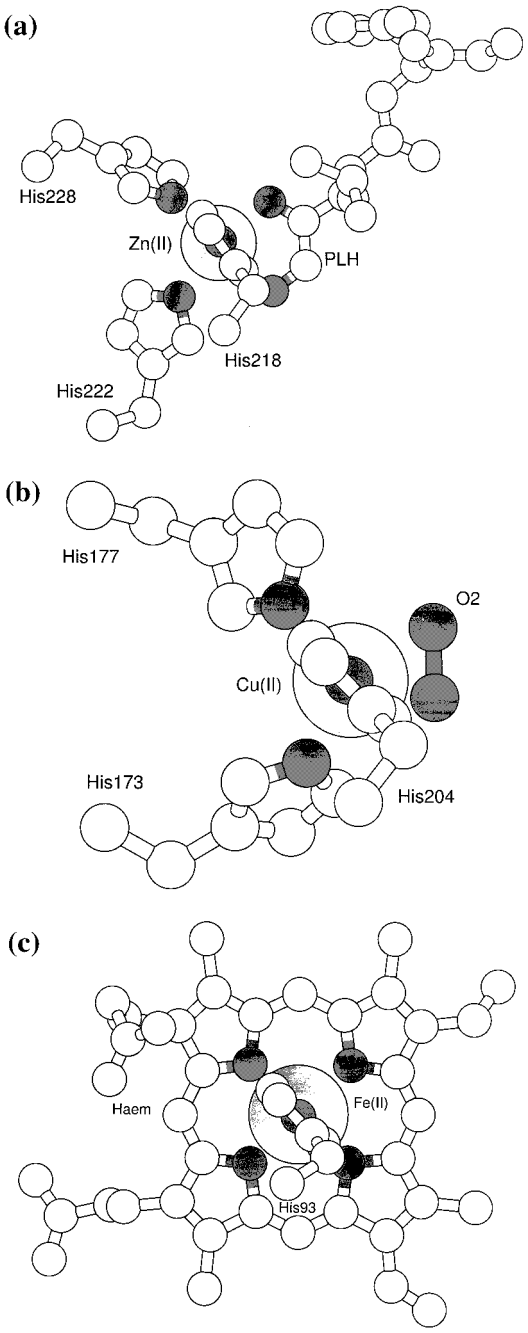

Figure 6. Conformation of the axial histidine residue in square pyramidal and octahedral coordination sites of divalent transition metal cations in natural metalloproteins according to X-ray crystallographic data: (a) neutrophil collagenase;[52] (b) hemocyanin;[78] (c) carbonmonoxymyoglobin.[86]

strate its high flexibility. Correspondingly, the barrier hindering the rotation of the aspartate anion is also expected to be small (around 4 kJ/mol) unless additional steric hindrances within NGF prevent this rotation, which has been evaluated by molecular modeling (discussed below).

Molecular Modeling. Because of limitations of the empirical force field molecular modeling approach, it is difficult to accurately determine structures of coordination sites in metallobiomolecules based exclusively on this approach, particularly for transition metal cations. Nevertheless, when combined with rigorous ab initio structural predictions, it has utility in assessing the size and flexibility of the coordination site and revealing factors that destabilize its structure.

CHARMM molecular mechanics calculations of the coordination site [M(N·His)$_3$($^-$O$_2$C$^{\gamma}$·Asp)] of NGF with selected transition metal cations result in similar three-dimensional structures. In all of these structures, four coordinating atoms, namely the carboxylate oxygens of Asp$^{105'}$, Nϵ of His^4, and Nδ of His$^{84'}$, lie approximately within the same plane forming a distorted square, with the fifth atom, Nϵ of His^8, "hanging over" and pulling the metal cation out of this plane. This particular geometry resembles a square base pyramidal coordination environment (structures **I-A** and **II-A**; Figures 2a and 3a) which is very common in metalloproteins,[43,50−53,77,78] while being rather unusual for Zn(II).[42,43]

The carboxylate group of Asp$^{105'}$ within the complexes has the C−O/C−C eclipsed conformation, which corresponds to the ab initio energy minimum as predicted by the present studies on propionate anion. Furthermore, this conformation of the aspartate anion is very rigid in the complexes, even though the carboxylate group itself is quite flexible within the frameworks of both ab initio and CHARMM force field descriptions. This conclusion is based on the energetics of the incremental rotation of the complexed and free carboxylate anion of Asp$^{105'}$ within NGF obtained with CHARMM force field calculations. Full structural relaxation of the coordination site (within the conformational space used) is taken into account for each particular conformation of the aspartate anion. For example, the barrier hindering the rotation of this group within the Zn(II)−NGF coordination site is found to be as high as 71 kJ/mol. Taking into account the empirical nature of the bioinorganic molecular mechanical force field, this value should not be taken literally. The obtained high barrier hindering the rotation of Asp$^{105'}$ demonstrates the rigidity of the coordination site such that the intrinsic inconsistency of transition metal cations with its particular geometry will result in its destruction, rather than in conformational alterations in Asp$^{105'}$.

The saddle-point of rotation of the aspartate anion in the complexes corresponds to the almost perpendicular conformation of the C−C and C−O bonds (torsional angle C−C−C−O is approximately −100°). In this conformation, the carboxyl group of Asp$^{105'}$, the Nϵ atom of His^8, and the metal cation lie approximately within the same plane, whereas chelating atoms Nϵ of His^4 and Nδ of His$^{84'}$ are located at the opposite sides of the plane. This geometry of the coordination site resembles a triangular bipyramidal environment (structures **I-B** and **II-B**; Figures 2b and 3b). The CHARMM potential energy decomposition reveals that the origin of the barrier of rotation of the aspartate anion in the complexes arises primarily from van der Waals repulsions of carboxylate oxygen atom from Nϵ of His^4 and chelated metal cation. It is essential to note that intrinsic stereochemical preferences of the transition metal cations are not considered in the CHARMM force field, hence the predicted hardening of rotation of the carboxyl anion is caused by steric hindrances inherent in the environment of the coordination site. Consequently, despite intrinsic flexibility of the carboxylate anion, the aspartate anion of Asp$^{105'}$ in the coordination site of NGF is unable to adopt the alternate conformation in response to the particular stereochemical preference of transition metal cations at reasonable temperatures.

The results of molecular modeling indicate that the coordination site within NGF possesses an inherent distorted square pyramidal geometry; thus, it is organized to chelate the transition metal cations which prefer this particular coordination environ-

(77) Fenton, D. E. *Biocoordination Chemistry*; Oxford University Press: Oxford, New York, Tokyo, 1995.

(78) Ton-That, H.; Magnus, K. *Protein Data Bank*; Brookhaven National Laboratory: Upton, NY; accession code 1OXY.

ment. Since transition metal cations demonstrate low affinities for NGF, one could predict that those metals which are not optimal for this environment, such as Co(II) and Rh(II) (Table 1), would not fit into this coordination site. This explains the striking lack of activity of Co(II), even though Co(II) has been established to closely match Zn(II) by radius and stereochemical preference in various coordination environments.[42,43,47,48] Furthermore, the ability of Pd(II) and Cu(II) to change conformation and modulate biological activities of NGF as effectively as Zn(II)[34,35] can be explained by the pronounced stereochemical preference of d^8 and d^9 metal cations toward the square pyramidal environment (Table 1).

Despite being compatible with a square pyramidal environment (Table 1), the only two exceptions, Ni(II) and Cd(II), do not demonstrate the biochemical and biological properties inherent in "fully active" ions, such as Zn(II), Cu(II), and Pd(II). Ni(II) affects only the TrkA-related activities of NGF, while Cd(II) appears to be inactive.[35] Therefore, selectivity of the NGF coordination site is governed by other factors in addition to the intrinsic stereochemical preference. Recent comprehensive studies on effects of transition metal cations on NGF activities have indicated that the "fully active" ions have intermediate radii whereas smaller and larger ions are inactive.[35] Consistent with this concept, present ab initio calculations of the model coordination complexes at the B3LYP/6-31+G* level demonstrate (Table 2) that the average metal−ligand separation is minimal for Ni(II) (2.082 and 2.062 Å for complexes **I** and **II**, respectively) and maximal for Cd(II) (2.339 and 2.329 Å); i.e., Ni(II) is indeed smaller while Cd(II) is larger than the "fully active" metal cations considered. The difference in metal−ligand separations seems to be small, but, because of the low affinity of transition metal cations for NGF, there exists high sensitivity of the affinity to all factors, particularly to the consistency of size (of the metal cations and the coordination site), which has been found to be very important in host−guest coordination chemistry.[79]

The CHARMM molecular mechanics calculations of the [M(N•His)$_3$($^-$O$_2$C$^\gamma$•Asp)] coordination site in NGF provide the structural basis for the observed size selectivity of NGF for transition metal cations. Table 3 presents deviations of the optimized geometries of the coordination site from the "ideal" structural features characteristic for complexes **I** and **II**. As seen, the increase of the radius of metal cation results in multiple structural distortions in the coordination site, which implies that the coordination complexes become less stable. The planarity of the base of the square pyramidal environment, and the coplanarity of metal cation with coordinating imidazole rings of residues His^4 and His$^{84'}$ are particularly sensitive to the increase of ionic radius of the cation. Hence, bulky cations, such as Cd(II) or Mn(II),[80] do not fit to the NGF coordination site because they would induce significant structural deformations.

Although the equilibrium structure of the coordination site seems to be most appropriate for Ni(II) in terms of satisfying the "ideal" geometric requirements (Table 3), the coordination site loses its rigidity since it cannot shrink sufficiently to accommodate this ion. Considerable loss of rigidity of the coordination site with enclosed Ni(II) is demonstrated by imposing its structural distortions followed by CHARMM energy refinement. The equilibrium distance between one of the coordinating residues and the metal cation was increased by 0.5 Å, and then the new distance was kept fixed while optimizing the remainder of the structure. No significant difference in the rigidity of the coordination site possessing Ni(II) with respect to the other metal cations was found when displacing residues His^4, His^8, and Asp$^{105'}$. On the other hand, detaching His$^{84'}$ from the coordination site requires much less energy for Ni (II) (about 6.3 kJ/mol) than for any other considered metal cation (more than 14.6 kJ/mol). This suggests that His$^{84'}$ cannot be tightly packed in the Ni(II)−NGF coordination complex. This particular residue is located in the rigid domain of NGF,[55] and therefore, it is not able to change its geometry enough to properly accommodate Ni(II).

Table 3. Deviations (C1−C5, Σ) of the Structural Elements of the [M(N•His)$_3$($^-$O$_2$C$^\gamma$•Asp)] Coordination Site within NGF for Transition Metal Cations from Corresponding "Ideal" Features (Inherent in Model Complexes I and II) as Predicted by CHARMM Force Field Calculations

cation M	radius,[a] Å	C1,[b] Å	C2,[c] Å	C3,[d] Å	C4,[e] Å	C5,[f] Å	Σ,[g] Å
Ni(II)	0.44	0.219	0.165	0.132	0.007	0.268	0.791
Cu(II)	0.57	0.240	0.139	0.199	0.006	0.354	0.939
Zn(II)	0.60	0.226	0.147	0.175	0.013	0.322	0.885
Pd(II)	0.64	0.269	0.131	0.220	0.017	0.362	1.000
Cd(II)	0.78	0.302	0.126	0.258	0.008	0.412	1.105

[a] Ionic radii of transition metal cations observed in four-coordinate environments in crystals.[80] [b] C1, deviation of a base of a pyramid of the square pyramidal environment of the metal from planarity; calculated as root-mean-square (rms) deviation of coordinating atoms of His^4, His,$^{84'}$ and Asp$^{105'}$ from the "best" plane. [c] C2, deviation of carboxylate anion of Asp$^{105'}$ from coplanarity with the metal; calculated as rms deviation of the CCO_2^- fragment of Asp$^{105'}$ and the cation from the "best" plane. [d] C3, deviation of imidazole ring of His^4 from coplanarity with the metal; calculated as rms deviation of atoms of the ring and the metal from the "best" plane. [e] C4, deviation of imidazole ring of His^8 from coplanarity with the metal; calculated as rms deviation of atoms of the ring and the metal from the "best" plane. [f] C5, deviation of imidazole ring of His$^{84'}$ from coplanarity with the metal; calculated as rms deviation of atoms of the ring and the metal from the "best" plane. [g] Σ, the sum of the rms deviations C1 through C5.

Consequently, we suggest that selectivity of the NGF coordination site for transition metal cations is determined by (i) its distinct square pyramidal geometry and (ii) its dimensions which best fit metal cations of intermediate sizes. Those transition metal cations which do not fit both criteria are not expected to form the fully coordinated state; however, they could form a state in which one or several NGF residues are substituted by water molecules. Experimental data indicate that this may be the case for Ni(II). This particular cation demonstrates inhibitory effects toward TrkA-mediated biological activities without affecting NGF protomer cross-linking nor p75^{NTR}-mediated activity.[35] High specificity of the effects of Ni(II) toward TrkA-mediated NGF activities is probably associated with the split of the NGF coordination site into two domains, with only one of them (responsible for TrkA-mediated activities) being affected by Ni(II). Since the split of the NGF coordination site has been predicted to be associated with the detaching of the amino terminus of NGF[33] and taking into account that this terminus constitutes a critical part of the TrkA receptor binding determinant,[8,57,58,81,82] we suggest that Ni(II) binds only to residues His^4 and His^8, thereby affecting the bioactive conformation of the terminus for TrkA activation.

Figure 7 illustrates putative conformations of free and complexed NGF obtained by CHARMM molecular modeling simulations in the framework of the present model. There are two essential features of this particular model. **First**, a putative NGF protomer cross-linking site (residues Ser^1 and Lys$^{115'}$;

(79) Cram, D. J. *Angew. Chem.* **1986**, *25*, 1039−1057.
(80) Shannon, R. D. *Acta Crystallogr.* **1976**, *A32*, 751−767.
(81) Kahle, P.; Burton, L. E.; Schmelzer, C. H.; Hertel, C. *J. Biol. Chem.* **1992**, *267*, 22707−22710.
(82) Shih, A.; Laramee, G. R.; Schmelzer, C. H.; Burton, L. E.; Winslow, J. W. *J. Biol. Chem.* **1994**, *269*, 27679−27686.

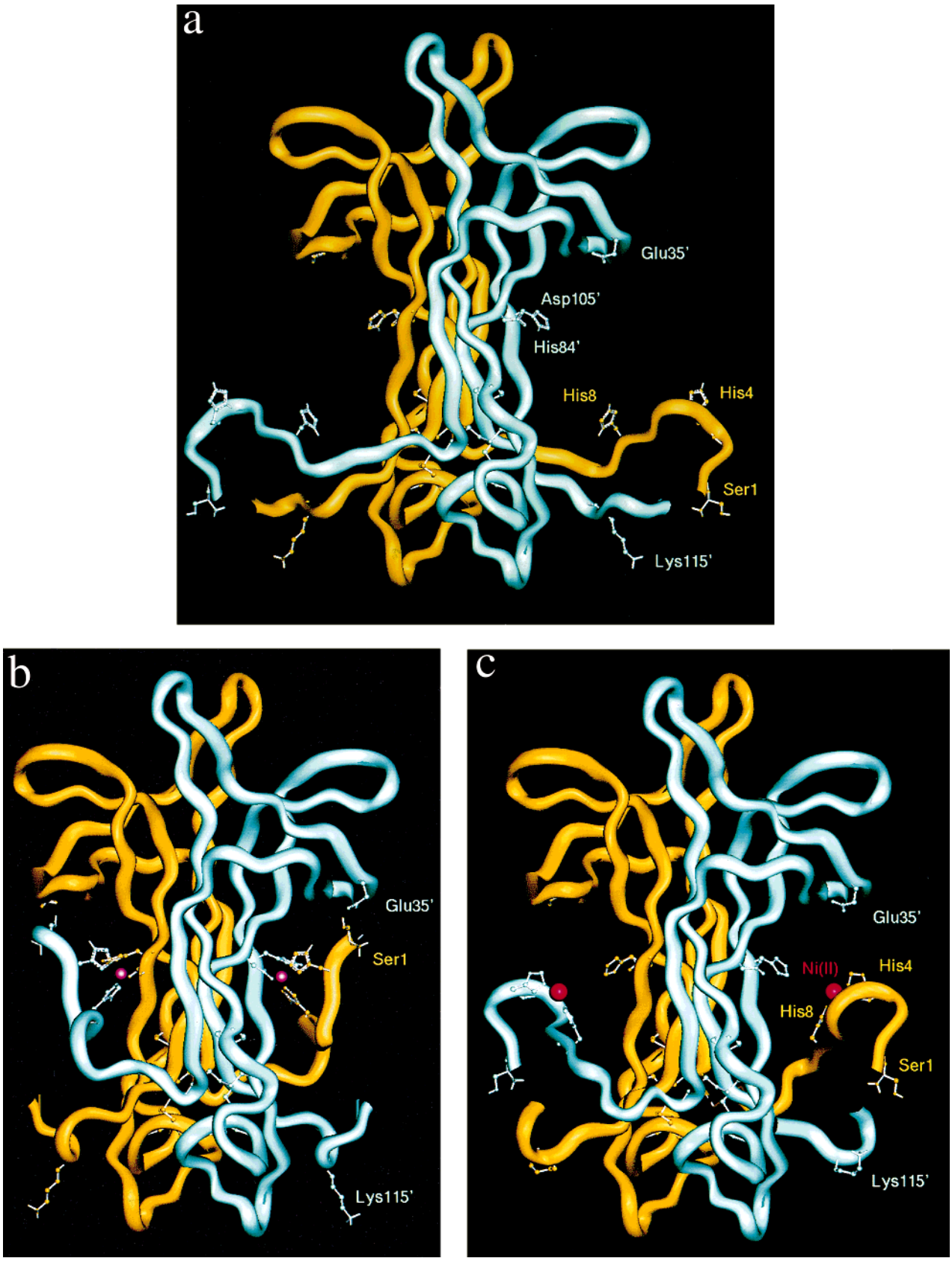

Figure 7. Equilibrium geometries of free and complexed NGF based on X-ray crystallography[54,55] and molecular modeling computations: (a) free NGF in predicted bioactive conformation;[57,58] (b) fully coordinated complex of NGF with Zn(II), Cu(II), or Pd(II), both TrkA and $p75^{NTR}$ binding determinants of NGF are affected and the protomer cross-linking site within NGF consisting of primary amines of Ser^{1} and $Lys^{115'}$ is lost; (c) partially coordinated complex of NGF with Ni(II) in which the protomer cross-linking site remains and only the TrkA binding determinant is affected. Yellow and blue colors designate different protomers of NGF; transition metal cations are shown as red spheres. Only residues essential for the discussion are denoted.

Figure 7)[33] is lost only in fully coordinated complexes when the amino terminus is detached from the juxtaposed carboxyl terminus (compare part b with parts a and c in Figure 7). **Second**, the $p75^{NTR}$ binding determinant (loops I and IV)[8,83−85] is altered only in fully coordinated complexes when the amino terminus creates steric hindrances in this area (Figure 7b). These features are consistent with available experimental data.[33−35] Thus, only metals which completely fit into the NGF coordination site by their stereochemical preference and size (Zn(II), Cu(II), and Pd(II)) display the full spectrum of biochemical and biological effects. Other transition metal cations display these effects only partially at best. Remarkably, there are no examples of metal cations which affect NGF protomer cross-linking without affecting its TrkA-mediated activities. Also, no metal cation which affects NGF/$p75^{NTR}$ binding without affecting TrkA-related activities has been found to date. These results suggest that compounds which bind to the amino/carboxyl terminal region of NGF may demonstrate selective TrkA effects.

Conclusions

A multidisciplinary approach including biochemical and theoretical methods has been utilized to explain the unusual selectivity of the metal coordination site within NGF. The most striking feature of this selectivity is that Co(II) and Cd(II), which behave similarly to Zn(II) in other metalloproteins, are inactive with respect to modulating NGF activities. Only Cu(II) and, to some extent Pd(II), possess the full spectrum of biochemical and biological activities characteristic of Zn(II). We suggest that the particular selectivity of the coordination site is caused by its five-coordinate distorted square pyramidal geometry which is uncommon for Zn(II)-containing proteins. Divalent transition metal cations are shown to split into three distinct groups: (i) those which prefer the square base pyramidal environment (d^8 elements Ni(II) and Pd(II)); (ii) those which are incompatible with the square pyramidal environment (d^7 elements Co(II) and Rh(II)); and (iii) those which have no or only minor intrinsic stereochemical preference (d^9 element Cu(II) and d^{10} elements Zn(II) and Cd(II)). Accordingly, the intrinsic stereochemical preference of Co(II) (d^7 element) in the pentacoordinated environment makes it inconsistent with the geometry of the coordination site within NGF. On the other hand, Cd(II) (d^{10} element) and Ni(II) (d^8 element), although stereochemically consistent with the square pyramidal coordination environment, are too large and too small to fit into the coordination site, respectively. Thus, the coordination site within NGF discriminates transition metal cations by their size and intrinsic stereochemical preference. The agreement between the observed selectivity of the NGF coordination site and theoretical predictions supports the suggested structure of this site. Because of the extreme importance of NGF as a survival factor in nerve cells, it is of striking significance that the selectivity of the metal coordination site within NGF is primarily limited to Zn(II) and Cu(II), i.e., to those transition metal cations which have been found in the brain in the highest concentrations, modulate functions of nerve cells, and most efficiently inhibit biological activities of NGF.

Acknowledgment. These studies are supported by the Medical Research Council of Canada, the Canadian Neuroscience Network Centre of Excellence, and the Heart and Stroke Foundation of Ontario (NA3718). G.M.R. is a Queen's National Scholar.

Note Added in Proof: Reference 30 (Van der Zee et al., 1996) has been retracted (*Science* **1999**, *285*, 340).

Supporting Information Available: (i) Atomic coordinates (in PDB format) of the free and complexed NGF, (ii) fully optimized total energies, and (iii) atomic coordinates (in Gaussian-94 input format) of the complexes $[M(NH_3)_3(^-O_2CCH_3)]$ and $[M(HNCH_2)_3(^-O_2CCH_3)]$ are available (PDF). This material is available free of charge via the Internet at http://pubs.acs.org.

JA983303Q

(83) Ibáñez, C. F.; Ebendal, T.; Barbany, G.; Murray-Rust, J.; Blundell, T. L.; Persson, H. *Cell* **1992**, *69*, 329−341.
(84) Ibáñez, C. F. *J. Neurobiol.* **1994**, *25*, 1349−1361.
(85) Shamovsky, I. L.; Ross, G. M.; Riopelle, R. J.; Weaver, D. F. *Protein Sci.* **1999**, *8*, in press.
(86) Vojtechovsky, J.; Berendzen, J.; Chu, K.; Schlichting, I.; Sweet, R. M. *Protein Data Bank*; Brookhaven National Laboratory: Upton, NY; accession code 1A6G.